Submitted Manuscript

Applied Spectroscopy

www.s-a-s.org

Recognition of Nucleophosmin Mutant Gene Expression of Leukemia Cells Using Raman Spectroscopy

Applied Spectroscopy
2023, Vol. 77(7) 689–697

DOI: 10.1177/00037028231176547
journals.sagepub.com/home/asp
Sage

Mingxin Li[1,2], Yihui Wu[1], Mingbo Chi[1], Yimeng Wang[1,2], Mingyao Zhu[1,2], and Sujun Gao[3]

Abstract

As a label-free, nondestructive, and in situ detection method, Raman spectroscopy analysis of single cells has potential application value in biomedical fields such as cancer diagnosis. In this study, the Raman spectral characteristics of nucleophosmin (NPM1)-mutant acute myeloid leukemia (AML) cells and nonmutated AML cells were investigated, and the reasons for the differences in spectral peaks were explained in combination with transcriptomic analysis. Raman spectra of two AML cell lines without NPM1 mutation (THP-1 and HL-60) and the OCI-AML3 cell line carrying the NPM1 mutant gene were cultured and collected experimentally. It was found that the average Raman spectra of NPM1 mutant and nonmutated cells had intensity differences in multiple peaks corresponding to chondroitin sulfate (CS), nucleic acid, protein, and other molecules. The differentially expressed genes were identified by quantitative analysis of the gene expression matrix of the two types of cells, and their roles in the regulation of CS proteoglycan and protein synthesis were analyzed. The results showed that the differences between the two types of cells expressed by the single-cell Raman spectral information were consistent with the differences in transcriptional profiles. This research could advance the application of Raman spectroscopy in cancer cell typing.

Keywords

Raman spectroscopy, acute myeloid leukemia cells, nucleophosmin, NPM1, mutation, transcriptome analysis

Date received: 10 November 2022; accepted: 30 March 2023

Introduction

Pathological diagnosis is mainly determined by morphology. Human cells or tissues are obtained through fine needle aspiration, surgical resection, endoscopic biopsy, etc., and a series of processing steps and observations of samples are conducted using microscopes and other tools to identify tumor cells according to their distribution and morphological structure. This diagnostic method is currently the "gold standard" for cancer diagnosis.[1] However, the process of sample preparation and staining is tedious and time-consuming and has many requirements for doctors. In addition, pathological diagnosis usually requires a combination of immunophenotyping, molecular genetics, and other detection methods to obtain the final diagnosis. These methods are not only expensive and time-consuming, but also rely on the experience of medical staff or involve a series of tests, and cancer does not show obvious symptoms during the early stage, making it difficult to ensure the accuracy of diagnosis.[2]

Cells are the basic units of all living organisms. Proteins, lipids, nucleic acids, and carbohydrates are important biological molecules that constitute cells. The composition and content of various biomolecules may change during the malignant transformation of cells, and these changes often occur much earlier than clinical symptoms. Raman spectroscopy can be used to detect these changes before they cause clinical manifestations and medical imaging abnormalities and can be used as an important detection method for early disease diagnosis and tumor grading.[3]

Raman spectroscopy is an inelastic scattering spectroscopy technique that is used to analyze molecular vibrational

[1]Changchun Institute of Optics, Fine Mechanics and Physics, Chinese Academy of Sciences, Changchun, China
[2]University of Chinese Academy of Sciences, Beijing, China
[3]Department of Hematology, The First Bethune Hospital of Jilin University, Changchun, China

Corresponding Authors:
Yihui Wu, Changchun Institute of Optics, Fine Mechanics and Physics, Chinese Academy of Sciences, Changchun, China.
Email: yihuiwu@ciomp.ac.cn

Mingbo Chi, Changchun Institute of Optics, Fine Mechanics and Physics, Chinese Academy of Sciences, Changchun, China.
Email: chimb@sklao.ac.cn

and rotational information. It has the advantages of label-free, nondestructive, and rapid detection. It can be used to detect the vibration of chemical bonds in cells and tissues and extract the spectral information of Raman active functional groups such as nucleic acids, proteins, lipids, and carbohydrates in single cells.[4] Raman spectroscopy can assist in evaluating, characterizing, and distinguishing cell types to provide objective and quantifiable molecular information for rapid clinical diagnosis and treatment. Therefore, Raman spectroscopy is widely used in the field of cancer diagnosis.[5–8]

Acute myeloid leukemia (AML) is an aggressive and refractory hematological malignancy characterized by the abnormal proliferation of immature myeloid cells in bone marrow and peripheral blood. Although the majority of AML patients achieve complete remission after chemotherapy and allogeneic hematopoietic stem cell transplantation, the five-year overall survival rate of AML patients remains low. Drug resistance and relapse are the two main factors that affect the survival of leukemia patients. Mutations in the nucleophosmin (NPM1) gene are one of the most common and clinically relevant genetic alterations in AML. Mutations in the NPM1 gene were detected in approximately 60% of patients with cytogenetically normal AML.[9,10] Due to its unique biological and clinical features, NPM1-mutated AML was defined as a distinct subtype of AML in the World Health Organization classification of leukemias.[11] Accurate identification of AML subtypes plays an important role in selecting treatment options and improving prognosis.

Transcriptomics provides important insights into gene structure, expression, and regulation and has been extensively studied in many organisms.[12–14] Transcriptome analysis is the key to understanding genome function and potential biological processes.[15] The objective of this study was to investigate the correlation between Raman spectroscopy and gene expression profiling. By comparing the transcriptome data of leukemia cells with the human reference genome and performing quantitative analysis of gene expression levels and differential expression analysis, differentially expressed genes were identified, and their biological processes were analyzed. Moreover, Raman spectroscopy was used to study the leukemia cell line with NPM1 mutation (OCI-AML3), and the THP-1 and HL-60 cell lines without NPM1 mutation, Raman spectral data were obtained, and the differences between the two were compared. The relationship between the transcriptome of leukemia cells and the cytochemical components corresponding to the Raman profile data was studied, and the Raman spectrum analysis data obtained from the leukemia cells were explained.

Materials and Methods

Cell Line Culture

The leukemia cell lines THP-1 and HL-60 were provided by the First Bethune Hospital of Jilin University, and the cell line OCI-AML3 carrying the NPM1 mutant gene was purchased from the Chinese Typical Culture Preservation Center of Wuhan University. The cell lines were cultured in RPMI 1640 medium containing 10% fetal bovine serum in a 5% CO_2-saturated humid incubator at 37 °C.

Raman Spectroscopy Acquisition

The cultured cells were placed on glass slides to prepare the test samples. The Raman spectra of single cells were collected by using the Raman spectrometer established in our laboratory. The 532 nm laser was selected as the excitation light source (Spectra-Physics Excelsior diode-pumped solid-state laser, 200 mW). After filtering and light intensity attenuation, the laser was focused on the cell surface through a 50 times microscope objective (Olympus). The focused spot size was 2 μm, and the power was approximately 35 mW. The recorded spectral range was 600–1800 cm^{-1}, and the integration time for spectral acquisition was 30 s. The resolution of the Raman spectrometer was approximately 2 cm^{-1}. As observed by using a microscope, these conditions did not burn cells while ensuring a sufficient signal-to-noise ratio. The frequency calibration of the spectrometer was performed using the 520.7 cm^{-1} silicon spectral line, and the standard deviation of the peak position shift was less than ±0.5 cm^{-1}. All measurements were performed in a dark room.

Spectral Data Processing

When the Raman spectral data of leukemia cells were collected, noise, glass substrate, fluorescence background, and other information interfere, which have a great impact on the quality of Raman spectra.[16–19] Therefore, it is necessary to preprocess the collected original Raman spectra before performing spectral data analysis.

First, the Savitzky–Golay filtering algorithm was used to smooth and denoise the spectral data. For the interference signals generated by the glass substrate, the specific-scale analysis algorithm based on wavelet transform was used to eliminate the influence of the substrate spectrum. Then, the background fluorescence was removed by the zero-order Savitzky–Golay filtering algorithm combined with the local minima.[20] Finally, the spectral signal intensity was normalized by the 1450 cm^{-1} Raman peak as a standard. The data preprocessing process was completed using Matlab R2019b (The MathWorks Inc.). The average spectra of leukemia cells with NPM1 mutation and without NPM1 mutation were plotted by Origin 2017 (OriginLab) software and the spectral differences between the two were analyzed and compared.

To evaluate whether the spectral differences between NPM1 mutant and nonmutant leukemia cells were statistically significant, IBM SPSS Statistics 29 software was used

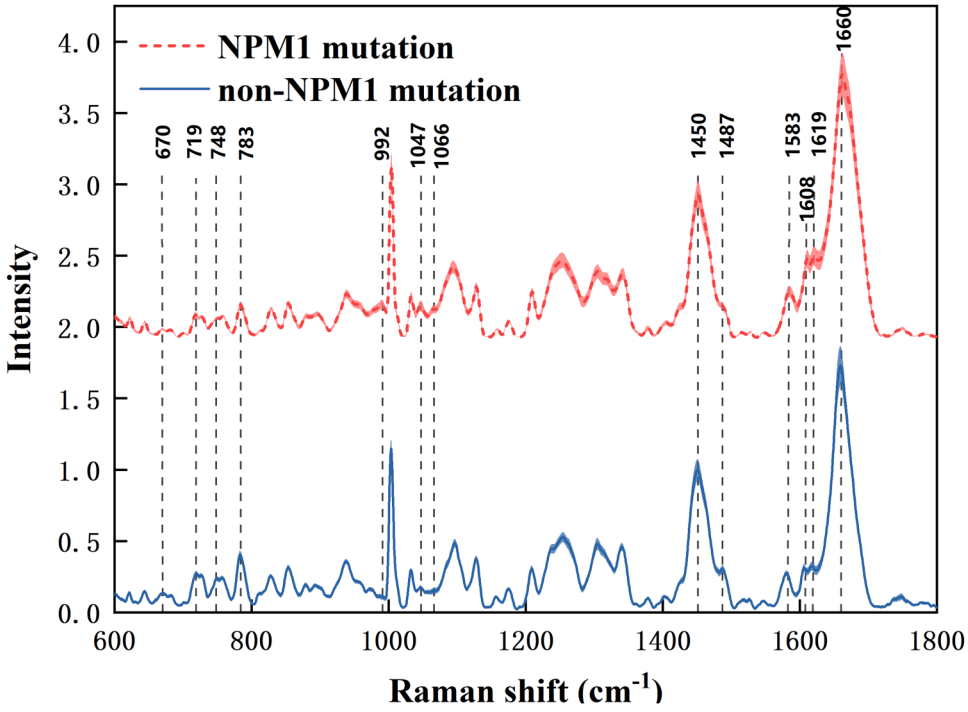

Figure 1. The averaged Raman spectra of NPM1 mutant leukemia cells and nonmutated leukemia cells. The upper red line represents the spectrum of the OCI-AML3 cell line carrying the NPM1 mutant gene. The following blue line represents the spectrum of the nonmutant leukemia cell lines THP-1 and HL-60. The shadow areas represent the 95% confidence intervals.

to perform an independent sample *t*-test on the spectral peak intensity values obtained from both groups that met the normality. For skewed spectral data, the nonparametric Mann–Whitney *U*-test was selected for comparison between groups. $P < 0.05$ indicated that the differences were statistically significant between the two groups of spectral data.

Transcriptomic Analysis

The gene expression data and clinical data of AML patients were obtained from the GSE6891 dataset in the Gene Expression Omnibus database, including 140 patients with NPM1 mutant leukemia and 317 leukemia patients without the NPM1-mutated genes. The linear models for microarray and RNA-sequenced data Limma method in R software was used to perform differential expression analysis using the two groups of data, and the Benjamini–Hochberg method was used to control the false discovery rate to obtain the adjusted *P* value.[21] Differentially expressed genes were identified using |log2 (Fold Change)| > 1 and adjusted *P* value < 0.05 as thresholds, and the results were visualized by volcano plot and box plots. The gene expression data obtained from the OCI-AML3, THP-1, and HL-60 leukemia cell lines were obtained from the Cancer Cell Line Encyclopedia (CCLE) database.

Results and Discussion

Comparison of Average Raman Spectra of Leukemia Cells

In this study, Raman spectra of AML cell lines were obtained from 186 samples, including 78 samples of THP-1 cells, 56 samples of HL-60 cells, and 52 samples of OCI-AML3 cells carrying the NPM1 mutation gene. The average Raman spectra obtained from the two types of cells with NPM1 mutation and those without NPM1 mutation are shown in Fig. 1. The diagram shows that the Raman spectra obtained from leukemia cells showed multiple spectral peaks in the range of the 600–1800 cm^{-1} fingerprint spectrum, which can fully reflect the changes in the content and composition of substances in different types of leukemia cells. The spectral differences between NPM1 mutant and nonmutant leukemia cells were mainly concentrated at 670 cm^{-1}, 719 cm^{-1}, 748 cm^{-1}, 783 cm^{-1}, 992 cm^{-1}, 1047 cm^{-1}, 1066 cm^{-1}, 1487 cm^{-1}, 1583 cm^{-1}, 1608 cm^{-1}, 1619 cm^{-1}, and 1660 cm^{-1}. The *P* value was calculated by an independent sample *t*-test or Mann–Whitney *U*-test and the differences in the above peaks were statistically analyzed (results shown in Fig. 2). The histogram results show that the spectral differences between leukemia cells with NPM1 mutation and those without NPM1 mutation were statistically significant ($P < 0.05$). The main spectral components of the cells and their designations are provided in Table 1.[22–27]

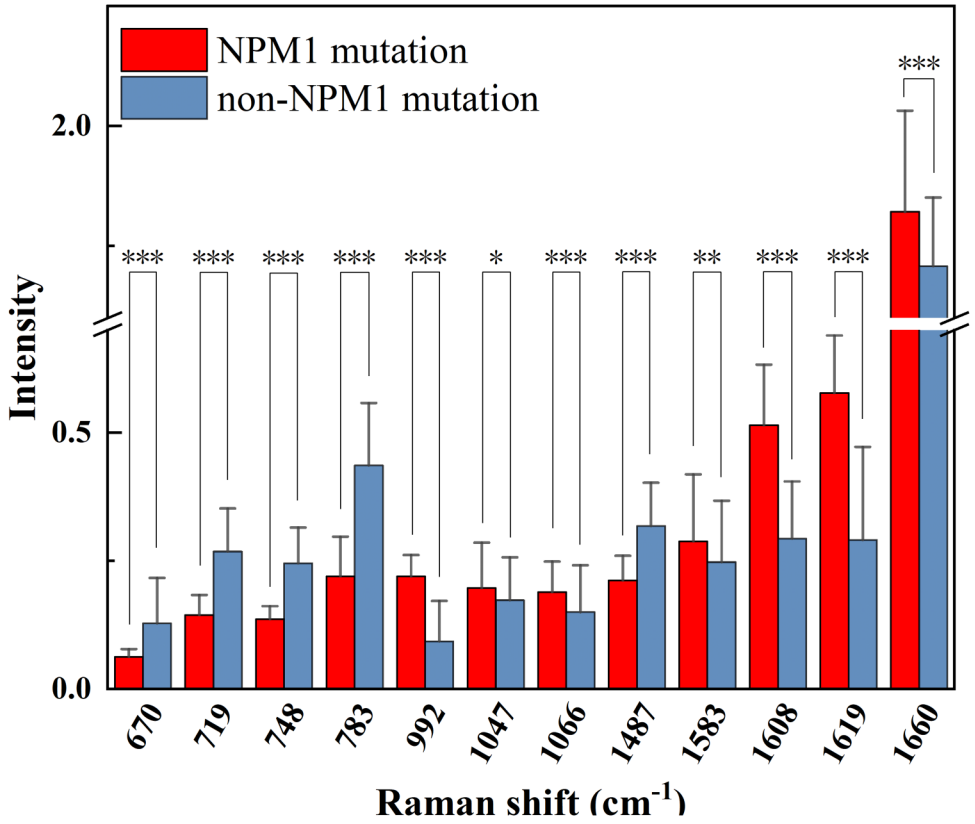

Figure 2. Histogram of NPM1 mutant and nonmutant leukemia cells. The spectral data conforming to a normal distribution are expressed as the mean value (standard deviation), while the data not conforming to a normal distribution are statistically described by the median (quartile). *P* values were calculated by independent sample *t*-test or Mann–Whitney *U*-test. $^{*}P < 0.05$, $^{**}P < 0.01$, $^{***}P < 0.001$.

Among these main differences, the Raman peaks at 1583 cm^{-1}, 1608 cm^{-1}, 1619 cm^{-1}, and 1660 cm^{-1} were mainly related to the proteins in the cells,[22,23,26,27] and the content in NPM1 mutant leukemia cells was significantly higher than that in nonmutant leukemia cells. Unlike the proteins, the signals of the Raman peaks at 670 cm^{-1}, 748 cm^{-1}, 783 cm^{-1}, and 1487 cm^{-1}, which might be related to nucleic acids,[22,23,26] were less intense in NPM1 mutant leukemia cells than in nonmutant cells. The decrease in the intensity of characteristic nucleic acid peaks may have been related to the genomic instability of NPM1 mutant leukemia cells.[28] We also found that the signals at 992 cm^{-1}, 1047 cm^{-1}, and 1066 cm^{-1} represented chondroitin sulfate (CS) in cells, and the content in NPM1 mutant leukemia cells was significantly higher than that in nonmutant leukemia cells.[24,25]

Differentially Expressed Genes

The Limma method in R software was used to identify differentially expressed genes in the gene expression dataset. Using |log2 (Fold Change)| > 1 and adjusted *P* value < 0.05 as screening conditions, a total of 136 differential genes were

Table I. Assignment of Raman spectrum peaks to biological molecules.

Peak position (cm^{-1})	Assignment	Composition	Reference
670	T, G	DNA/RNA	22
719	$CN^{+}(CH_3)_3$ stretching	Lipids	22
748	Thymine ring breathing mode	Nucleic acids	23
783	U, C, T ring breathing	DNA/RNA	22
992	C–O–S	CS	24
1047	C–OH	CS	25
1066	OSO_3^-	CS	24
1450	CH_2, CH_3 deformation/ CH_2 vibration	Proteins/lipids	26,27
1487	A, G	Nucleic acids	26
1583	C=C bending, phenylalanine	Proteins	23
1608	Phenylalanine, tyrosine, C=C	Proteins	22,26
1619	Tyrosine, tryptophan, C=C stretching mode	Proteins	22,26
1660	Amide I (α-helix)	Proteins	27

identified, of which 79 were upregulated and 57 were downregulated in NPM1 mutant leukemia samples (Fig. 3). We selected several genes that had expression levels that were significantly different and that have been confirmed to be closely related to NPM1 mutant leukemia and visualized the results by box plots (Fig. 4).[29–34]

The box plots show that HOX genes such as HOXA10 and HOXB6 were highly expressed in NPM1 mutant cells. HOX genes are important regulatory factors of embryonic and hematopoietic cell development, and their overexpression is associated with leukemogenesis.[29] The HOX locus also contains lncRNAs involved in cell differentiation and cancer pathogenesis.[35–40] HOXB-AS3 is a long noncoding RNA (lncRNA) embedded in the HOXB locus that plays a role in regulating ribosomal RNA (rRNA) transcription and ribosome biogenesis in leukemia cells. It was highly expressed in NPM1 mutant cells. The HOX gene often functions synergistically with other genes, the most common of which is the MEIS1 gene. The MEIS1 gene was significantly upregulated in NPM1 mutant leukemia cells. As a transcription factor, the MEIS1 gene can combine with the HOX gene to form a dimer to accelerate the occurrence of AML.[30] The VCAN gene, which is a member of the proteoglycan family, was highly expressed in NPM1 mutant cells. It was reported that inhibition of VCAN expression can significantly reduce the invasion ability of leukemia cells.[31] The expression of the CD34 gene was upregulated in nonmutant cells. CD34 is a highly glycosylated cell surface antigen that can inhibit the differentiation of myeloid cells and cause them to stay in the early hematopoietic stage.

Differential Genes Expressions in Cell Lines

The leukemia cell line OCI-AML3 carries the NPM1 mutant gene. It has the molecular and biological characteristics of NPM1 mutant AML and is an important tool for studying this AML subtype.[41] The gene expression data of three AML cell lines (OCI-AML3, THP-1, and HL-60) were obtained from the CCLE database, and the expression differences in the HOXA10, HOXB6, HOXB-AS3, VCAN, MEIS1, and CD34 genes in leukemia cell lines were analyzed. As shown in Fig. 5, the HOXA10, HOXB6, HOXB-AS3, VCAN, and MEIS1 genes were highly expressed in the OCI-AML3 cell line with NPM1 mutation, while the expression of CD34 was not obviously different among the three cell lines. Comparing the gene expression data shown in Figs. 4 and 5 revealed that the differentially expressed gene results obtained in leukemia cell lines and clinical samples were consistent. Studying the biological and genetic characteristics of leukemia cell lines is of great clinical value for the diagnosis and classification of AML.

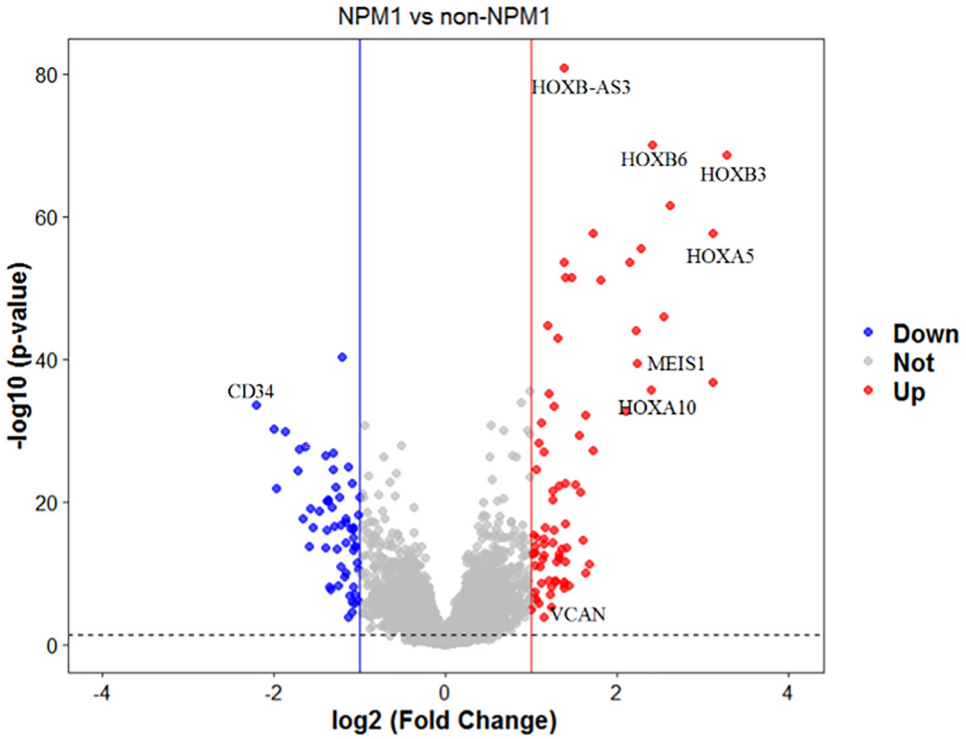

Figure 3. Volcano plot of differentially expressed genes in clinical samples. The thresholds for differentially expressed genes were |log2 (Fold Change)| > 1 and adjusted *P* value < 0.05. The red points on the right represent upregulated differentially expressed genes in NPM1-mutated leukemia samples. The blue points on the left represent downregulated differentially expressed genes.

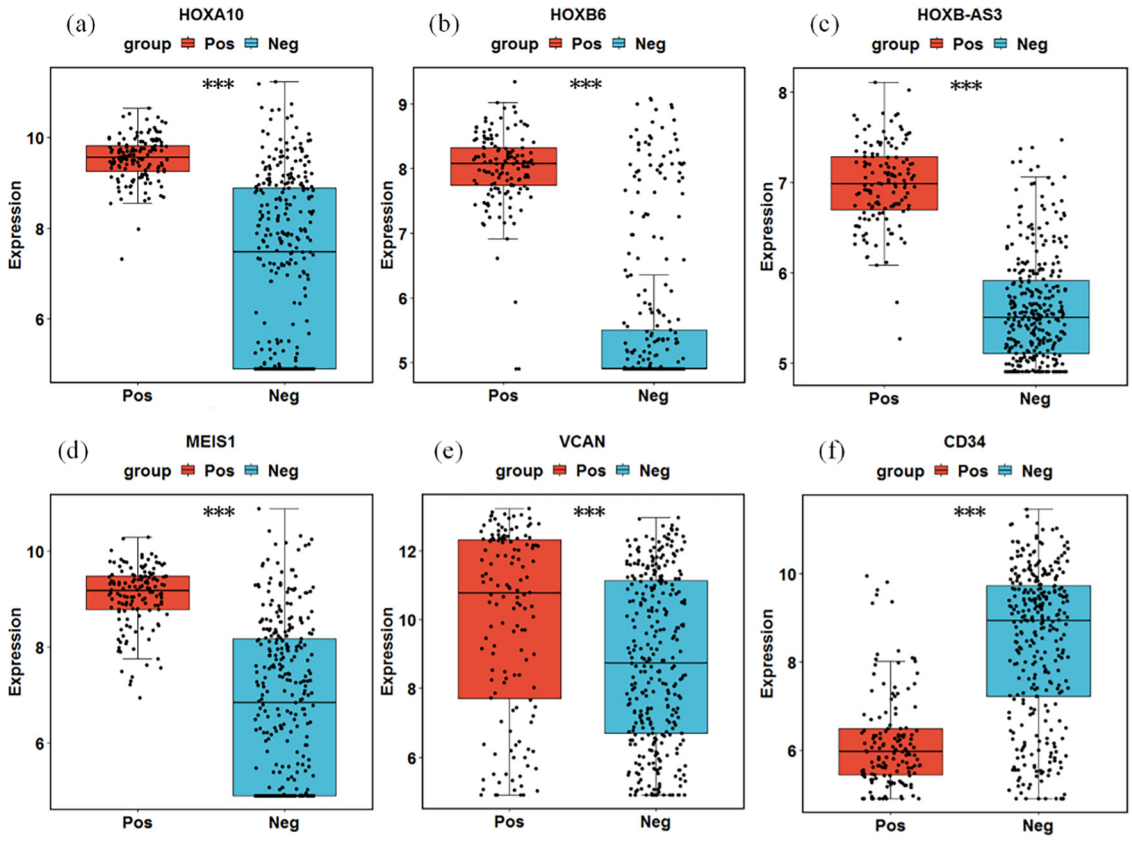

Figure 4. Boxplots of differentially expressed genes in clinical samples. The expression of the (a) HOXA10, (b) HOXB6, (c) HOXB-AS3, (d) MEIS1, (e) VCAN, (f) and CD34 genes in NPM1 mutant and nonmutant leukemia cells. Pos represents the NPM1 mutant leukemia group, and Neg represents the nonmutant leukemia group.

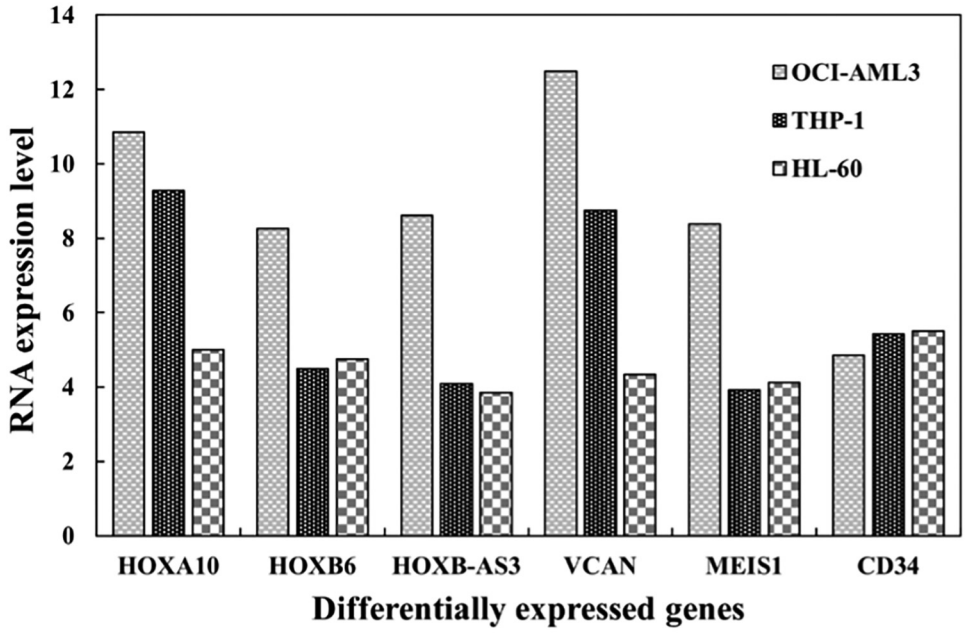

Figure 5. Expression of differential genes in leukemia cell lines. OCI-AML3 is a leukemia cell line carrying the NPM1 mutant gene. THP-1 and HL-60 are leukemia cell lines without the NPM1 mutant gene.

Discussion

Genes were differentially expressed in different types of AML, and their expression levels were closely related to AML classification. HOX genes are a family of transcription factors containing homologous domains. There are 39 genes in total, which can be divided into four clusters: A, B, C, and D. These gene clusters were found to be located on chromosomes 7, 17, 12, and 2, respectively.[42,43] There are some lncRNA genes in the noncoding region between HOX genes, which play an important role in regulating the expression of HOX genes that encode proteins. Studies have shown that HOX genes are overexpressed in AML with NPM1 mutations.[32,33] HOXA10 can promote the proliferation of bone marrow hematopoietic progenitor cells (HPCs) and AML cells by upregulating the expression of the target gene FGF2.[44] The HOXB6 gene can promote the proliferation of HPCs and inhibit their differentiation. HOXB-AS3 is a lncRNA within the HOXB locus and is one of the most highly expressed lncRNAs in AML patients with NPM1 mutations. The upregulation of HOXB-AS3 was found to be driven by mutations in NPM1. HOXB-AS3 has been shown to interact with ErbB3 binding protein 1 (EBP1) and guide EBP1 to ribosomal DNA sites, enhancing the interaction between EBP1 and NPM1 and increasing the production of transcribed rRNA. Through this mechanism, HOXB-AS3 regulates ribosomal RNA transcription and improves protein translation efficiency in a state of increasing metabolic demand.[34]

The VCAN gene encodes a macromolecular CS proteoglycan. The high expression of VCAN was found to be regulated by the NPM1 mutant protein-mediated transforming growth factor-β/cytoplasmic promyelocytic leukemia/Smad signaling pathway.[31] VCAN can increase the invasion and metastasis of tumor cells by activating nuclear factor-κB signaling and upregulating the hyaluronic acid receptor CD44, receptor of hemagglutinin-mediated motility, and matrix metalloproteinase 9.[45–47] The epidermal growth factor-like motif in the G3 domain of VCAN binds to the epidermal growth factor receptor (EGFR) and activates the EGFR-phosphoinositide 3-kinase-Akt-mammalian target of rapamycin pathway, promoting cell proliferation and protein synthesis.[48–50]

In the Raman spectroscopy results, the signals at 1583 cm^{-1}, 1608 cm^{-1}, 1619 cm^{-1}, and 1660 cm^{-1} corresponded to the phenylalanine/C=C bending mode, phenylalanine/tyrosine/C=C, the tyrosine/tryptophan/C=C stretching mode and amide I (α-helix), respectively. The peak intensity of these Raman peaks characterizing proteins was significantly higher in NPM1 mutant leukemia cells than in nonmutant cells, which was consistent with our transcriptome analysis results. In addition, three characteristic peaks at 992 cm^{-1} (C–O–S), 1047 cm^{-1} (C–OH), and 1066 cm^{-1} (OSO_3^-) were related to CS in cells. The high expression of the VCAN gene in NPM1 mutant leukemia cells explained why the intensity of CS-related Raman peaks was higher in these cells than in nonmutant cells.

Raman spectroscopy can be used to obtain information on molecular structure, chemical composition, and molecular interactions in cells and tissues, so it can be used for differential diagnosis of diseases.[51] Raman spectroscopy has the advantages of less water interference and label-free, nondestructive detection and can be used to study the molecular characteristics of living cells. Raman spectroscopy data are mainly analyzed by multivariate statistical analysis methods such as principal component analysis and linear discriminant analysis.[52,53] While these methods can sometimes successfully distinguish spectra from different cell types or states, the interpretation of the results remains unclear because they do not provide insights into the biological mechanisms underlying spectral differences. In this study, cell Raman spectroscopy data were linked to transcriptomic data, and the reasons for the differences in Raman spectroscopy data from different types of cells were revealed through the study of gene expression. Our research showed that single-cell Raman spectroscopy had the potential to be used to obtain omics information from living cells in a nondestructive way and had important clinical application value.

Conclusion

In this study, a homemade high-resolution Raman spectrometer was used to analyze the Raman spectra and corresponding transcriptome data of leukemia cells with NPM1 mutation and cells without NPM1 mutation. The results showed that there were significant differences in their Raman spectra at 992 cm^{-1}, 1047 cm^{-1}, 1066 cm^{-1}, 1583 cm^{-1}, 1608 cm^{-1}, 1619 cm^{-1}, and 1660 cm^{-1}. These differences were consistent with the changes in CS proteoglycan and protein synthesis regulated by VCAN and HOX genes driven by the NPM1 mutant gene. The Raman spectra of AML cells were related to cell gene expression profiles. The combination of cellular Raman spectroscopy and transcriptomics can promote the understanding of single-cell Raman spectra from the perspective of molecular biological mechanisms. This method could be helpful to solve the problems of subjective histopathology and the accurate identification of cell subtypes and could be of great importance for the early screening of cancer and selection of initial treatment options.

Declaration of Conflicting Interests

The author(s) declared no potential conflicts of interest with respect to the research, authorship, and/or publication of this article.

Funding

The author(s) disclosed receipt of the following financial support for the research, authorship, and/or publication of this article: This work was supported by the National Natural Science Foundation of China (U21A20395, 61727813), Research Equipment Development Project of the Chinese Academy of Sciences

(YJKYYQ20210035), and Bethune Medical Engineering and Instruments Centre Fund (BQEGCZX2021010).

ORCID iDs

Yihui Wu https://orcid.org/0000-0002-5289-3766
Mingbo Chi https://orcid.org/0000-0001-8683-4257

References

1. K. Kong, C.J. Rowlands, S. Varma, W. Perkins, et al. "Diagnosis of Tumors During Tissue-Conserving Surgery with Integrated Autofluorescence and Raman Scattering Microscopy". Proc. Natl. Acad. Sci. U.S.A. 2013. 110(38): 15189–15194. 10.1073/pnas.1311289110
2. M. Paraskevaidi, B.J. Matthew, B.J. Holly, B.J. Hugh, et al. "Clinical Applications of Infrared and Raman Spectroscopy in the Fields of Cancer and Infectious Diseases". Appl. Spectrosc. Rev. 2021. 56(8-10): 804–868. 10.1080/05704928.2021.1946076
3. K. Hanna, E. Krzoska, A.M. Shaaban, D. Muirhead, et al. "Raman Spectroscopy: Current Applications in Breast Cancer Diagnosis, Challenges and Future Prospects". Br. J. Cancer. 2022. 126(8): 1125–1139. 10.1038/S41416-021-01659-5
4. S. Managò, G. Zito, A.C. De Luca. "Raman Microscopy Based Sensing of Leukemia Cells: A Review". Opt. Laser Technol. 2018. 108: 7–16. 10.1016/j.optlastec.2018.06.034
5. E. Barroso, R. Smits, T. Bakker Schut, I. Ten Hove, et al. "Discrimination Between Oral Cancer and Healthy Tissue Based on Water Content Determined by Raman Spectroscopy". Anal. Chem. 2015. 87(4): 2419–2426. 10.1021/ac504362y
6. R.E. Kast, S.C. Tucker, K. Killian, M. Trexler, et al. "Emerging Technology: Applications of Raman Spectroscopy for Prostate Cancer". Cancer Metastasis Rev. 2014. 33(2): 673–693. 10.1007/S10555-013-9489-6
7. M. Li, S.R. Banerjee, C. Zheng, M.G. Pomper, et al. "Ultrahigh Affinity Raman Probe for Targeted Live Cell Imaging of Prostate Cancer". Chem. Sci. 2016. 7(11): 6779–6785. 10.1039/C6SC01739H
8. L. Li, J. Yang, J. Wei, C. Jiang, et al. "SERS Monitoring of Photoinduced-Enhanced Oxidative Stress Amplifier on Au@Carbon Dots for Tumor Catalytic Therapy". Light: Sci. Appl. 2022. 11(1): 1–11. 10.1038/S41377-022-00968-5
9. B. Falini, C. Mecucci, E. Tiacci, M. Alcalay, et al. "Cytoplasmic Nucleophosmin in Acute Myelogenous Leukemia with a Normal Karyotype". N. Engl. J. Med. 2005. 352(3): 254–266. 10.1056/nejmoa041974
10. H. Becker, G. Marcucci, K. Maharry, M.D. Radmacher, et al. "Favorable Prognostic Impact of NPM1 Mutations in Older Patients with Cytogenetically Normal De Novo Acute Myeloid Leukemia and Associated Gene- and MicroRNA-Expression Signatures: A Cancer and Leukemia Group B Study". J. Clin. Oncol. 2010. 28(4): 596–604. 10.1200/JCO.2009.25.1496
11. D.A. Arber, A. Orazi, R. Hasserjian, J. Thiele, et al. "The 2016 Revision to the World Health Organization Classification of Myeloid Neoplasms and Acute Leukemia". Blood. 2016. 127 (20): 2391–2405. 10.1182/blood-2016-03-643544
12. A. Casamassimi, A. Federico, M. Rienzo, S. Esposito, et al. "Transcriptome Profiling in Human Diseases: New Advances and Perspectives". Int. J. Mol. Sci. 2017. 18(8): 1652. 10.3390/ijms18081652
13. M. Jain. "Next-Generation Sequencing Technologies for Gene Expression Profiling in Plants". Briefings Funct. Genomics. 2012. 11(1): 63–70. 10.1093/Bfgp/Elr038
14. R. Lowe, N. Shirley, M. Bleackley, S. Dolan, et al. "Transcriptomics Technologies". PLoS Comput. Biol. 2017. 13(5): E1005457. 10.1371/journal.pcbi.1005457
15. J.A. Martin, Z. Wang. "Next-Generation Transcriptome Assembly". Nat. Rev. Genet. 2011. 12(10): 671–682. 10.1038/nrg3068
16. D. Wei, S. Chen, Q. Liu. "Review of Fluorescence Suppression Techniques in Raman Spectroscopy". Appl. Spectrosc. Rev. 2015. 50(5): 387–406. 10.1080/05704928.2014.999936
17. H.J. Byrne, P. Knief, M.E. Keating, F. Bonnier. "Spectral Pre and Post Processing for Infrared and Raman Spectroscopy of Biological Tissues and Cells". Chem. Soc. Rev. 2016. 45(7): 1865–1878. 10.1039/C5CS00440C
18. E. Barroso, T. Bakker Schut, P. Caspers, I. Santos, et al. "Characterization and Subtraction of Luminescence Background Signals in High-Wavenumber Raman Spectra of Human Tissue". J. Raman Spectrosc. 2018. 49(4): 699–709. 10.1002/Jrs.5338
19. D.W. Shipp, F. Sinjab, I. Notingher. "Raman Spectroscopy: Techniques and Applications in the Life Sciences". Adv. Opt. Photon. 2017. 9(2): 315–428. 10.1364/AOP.9.000315
20. X. Han, Y. Wu, M. Chi, S. Gao, Q. Wang. "Single-Cell Raman Spectrum Extraction from Clinic Biosamples". J. Raman Spectrosc. 2020. 51(11): 2255–2264. 10.1002/Jrs.5984
21. Y. Benjamini, Y. Hochberg. "Controlling the False Discovery Rate: A Practical and Powerful Approach to Multiple Testing". J. R. Stat. Soc. B. 1995. 57(1): 289–300. 10.1111/J.2517-6161.1995.Tb02031.X
22. I. Notingher, L.L. Hench. "Raman Microspectroscopy: A Noninvasive Tool for Studies of Individual Living Cells in Vitro". Expert Rev. Med. Devices. 2006. 3(2): 215–234. 10.1586/17434440.3.2.215
23. S. Chai, X. Sun, C. Fu, Q. Xu, et al. "Identification and Characterization of the Inhibitory Effect of ART on Colorectal Cancer Cells Using Raman Spectroscopy". J. Raman Spectrosc. 2022. 53(2): 191–201. 10.1002/Jrs.6292
24. R. Ellis, E. Green, C.P. Winlove. "Structural Analysis of Glycosaminoglycans and Proteoglycans by Means of Raman Microspectrometry". Connect. Tissue Res. 2009. 50(1): 29–36. 10.1080/03008200802398422
25. R. Bansil, I. Yannas, H. Stanley. "Raman Spectroscopy: A Structural Probe of Glycosaminoglycans". Biochim. Biophys. Acta, Gen. Subj. 1978. 541(4): 535–542. 10.1016/0304-4165(78)90163-0
26. J.W. Chan, D.S. Taylor, T. Zwerdling, S.M. Lane, et al. "Micro-Raman Spectroscopy Detects Individual Neoplastic and Normal Hematopoietic Cells". Biophys. J. 2006. 90(2): 648–656. 10.1529/Biophysj.105.066761
27. J. Tang, Y. Bao, J. Wu, L. Shang, et al. "Study on Breast Tissue Cancerization by Polarized Micro-Raman Spectroscopy". Chin. J. Anal. Chem. 2021. 49(12): 2048–2054. 10.19756/J.Issn.0253-3820.210602
28. C. Vascotto, L. Lirussi, M. Poletto, M. Tiribelli, et al. "Functional Regulation of the Apurinic/Apyrimidinic Endonuclease 1 by

Nucleophosmin: Impact on Tumor Biology". Oncogene. 2014. 33(22): 2876–2887. 10.1038/Onc.2013.251
29. B. Falini, L. Brunetti, P. Sportoletti, M.P. Martelli. "NPM1-Mutated Acute Myeloid Leukemia: From Bench to Bedside". Blood. 2020. 136(15): 1707–1721. 10.1182/Blood.2019004226
30. U. Thorsteinsdottir, E. Kroon, L. Jerome, F. Blasi, G. Sauvageau. "Defining Roles for HOX and MEIS1 Genes in Induction of Acute Myeloid Leukemia". Mol. Cell. Biol. 2001. 21(1): 224–234. 10.1128/MCB.21.1.224-234.2001
31. L. Yang, L. Wang, Z. Yang, H. Jin, et al. "Up-Regulation of EMT-Related Gene VCAN by NPM1 Mutant-Driven TGF-B/cPML Signalling Promotes Leukemia Cell Invasion". J. Cancer. 2019. 10(26): 6570–6583. 10.7150/Jca.30223
32. M. Alcalay, E. Tiacci, R. Bergomas, B. Bigerna, et al. "Acute Myeloid Leukemia Bearing Cytoplasmic Nucleophosmin (NPMc + AML) Shows a Distinct Gene Expression Profile Characterized by Up-Regulation of Genes Involved in Stem-Cell Maintenance". Blood. 2005. 106(3): 899–902. 10.1182/Blood-2005-02-0560
33. L. Brunetti, M.C. Gundry, D. Sorcini, A.G. Guzman, et al. "Mutant NPM1 Maintains the Leukemic State Through HOX Expression". Cancer Cell. 2018. 34(3): 499–512.e9. 10.1016/J.Ccell.2018.08.005
34. D. Papaioannou, A. Petri, O.M. Dovey, S. Terri, et al. "The Long Non-Coding RNA HOXB-AS3 Regulates Ribosomal RNA Transcription in NPM1-Mutated Acute Myeloid Leukemia". Nat. Commun. 2019. 10(1): 1–15. 10.1038/S41467-019-13259-2
35. R.A. Gupta, N. Shah, K.C. Wang, J. Kim, et al. "Long Non-Coding RNA HOTAIR Reprograms Chromatin State to Promote Cancer Metastasis". Nature. 2010. 464(7291): 1071–1076. 10.1038/Nature08975
36. M. Huarte. "The Emerging Role of lncRNAs in Cancer". Nat. Med. 2015. 21(11): 1253–1261. 10.1038/nm.3981
37. E. Leucci, R. Vendramin, M. Spinazzi, P. Laurette, et al. "Melanoma Addiction to the Long Non-Coding RNA SAMMSON". Nature. 2016. 531(7595): 518–522. 10.1038/Nature17161
38. A. Schwarzer, S. Emmrich, F. Schmidt, D. Beck, et al. "The Non-Coding RNA Landscape of Human Hematopoiesis and Leukemia". Nat. Commun. 2017. 8(1): 1–17. 10.1038/S41467-017-00212-4
39. T. Trimarchi, E. Bilal, P. Ntziachristos, G. Fabbri, et al. "Genome-Wide Mapping and Characterization of Notch-Regulated Long Noncoding RNAs in Acute Leukemia". Cell. 2014. 158(3): 593–606. 10.1016/J.Cell.2014.05.049
40. X. Yan, Z. Hu, Y. Feng, X. Hu, et al. "Comprehensive Genomic Characterization of Long Non-Coding RNAs Across Human Cancers". Cancer Cell. 2015. 28(4): 529–540. 10.1016/J.Ccell.2015.09.006
41. H. Quentmeier, M. Martelli, W. Dirks, N. Bolli, et al. "Cell Line OCI/AML3 Bears Exon-12 NPM Gene Mutation-A and Cytoplasmic Expression of Nucleophosmin". Leukemia. 2005. 19(10): 1760–1767. 10.1038/Sj.Leu.2403899
42. N. Shah, S. Sukumar. "The Hox Genes and Their Roles in Oncogenesis". Nat. Rev. Cancer. 2010. 10(5): 361–371. 10.1038/Nrc2826
43. K.L. Rice, J.D. Licht. "HOX Deregulation in Acute Myeloid Leukemia". J. Clin. Invest. 2007. 117(4): 865–868. 10.1172/JCI31861
44. C.A. Shah, L. Bei, H. Wang, L.C. Platanias, E.A. Eklund. "Hoxa10 Protein Regulates Transcription of Gene Encoding Fibroblast Growth Factor 2 (FGF2) in Myeloid Cells". J. Biol. Chem. 2012. 287(22): 18230–18248. 10.1074/Jbc.M111.328401
45. P.A. Keire, I. Kang, T.N. Wight. "Versican: Role in Cancer Tumorigenesis". In: R. Brekken, D. Stupack, editors. Extracellular Matrix in Tumor Biology. Berlin, Germany: Springer, Cham, 2017. Pp. 51–74. 10.1007/978-3-319-60907-2_4
46. T.-L. Yeung, C.S. Leung, K.-K. Wong, G. Samimi, et al. "TGF-B Modulates Ovarian Cancer Invasion by Upregulating CAF-Derived Versican in the Tumor Microenvironment". Cancer Res. 2013. 73(16): 5016–5028. 10.1158/0008-5472.CAN-13-0023
47. A. Papadas, G. Arauz, A. Cicala, J. Wiesner, F. Asimakopoulos. "Versican and Versican-Matrikines in Cancer Progression, Inflammation, and Immunity". J. Histochem. Cytochem. 2020. 68(12): 871–885. 10.1369/0022155420937098
48. G. Zhangyuan, F. Wang, H. Zhang, R. Jiang, et al. "Versicanv1 Promotes Proliferation and Metastasis of Hepatocellular Carcinoma Through the Activation of EGFR–PI3K–AKT Pathway". Oncogene. 2020. 39(6): 1213–1230. 10.1038/S41388-019-1052-7
49. Y. Mesbahi, T.N. Trahair, R.B. Lock, P. Connerty. "Exploring the Metabolic Landscape of AML: From Haematopoietic Stem Cells to Myeloblasts and Leukaemic Stem Cells". Front. Oncol. 2022. 12: 807266. 10.3389/Fonc.2022.807266
50. H. Liang, X. Cheng, W. Yang, W. Yu, et al. "Raman Spectral Characteristics of Human Embryonic Stem Cells and Acute Promyelocytic Leukemia Cells". Guang Pu Xue Yu Guang Pu Fen Xi [Spectrosc. Spectral Anal.]. 2020. 40(1): 1–9. 10.3964/j.issn.1000-0593(2020)01-0001-09
51. G.B. Jung, S.W. Kang, G.-J. Lee, D. Kim. "Biochemical Characterization of the Brain Hippocampal Areas After Cerebral Ischemia-Reperfusion Using Raman Spectroscopy". Appl. Spectrosc. 2018. 72(10): 1479–1486. 10.1177/0003702818776627
52. W. Liu, Z. Sun, J. Chen, C. Jing. "Raman Spectroscopy in Colorectal Cancer Diagnostics: Comparison of PCA-LDA and PLS-DA Models". J. Spectrosc. 2016. 2016: Article ID 1603609. 10.1155/2016/1603609
53. H. Liang, X. Cheng, S. Dong, H. Wang, et al. "Rapid and Non-Invasive Discrimination of Acute Leukemia Bone Marrow Supernatants by Raman Spectroscopy and Multivariate Statistical Analysis". J. Pharm. Biomed. Anal. 2022. 210: 114560. 10.1016/J.Jpba.2021.114560